

BURSTS OF EXTENSIVE AIR SHOWERS: CHAOS VS. STOCHASTICITY

Yu.A. Fomin^{*}, G.V. Kulikov, M.Yu. Zotov

Ultrahigh Energy Particles Laboratory, D. V. Skobeltsyn Institute of Nuclear Physics, M. V. Lomonosov Moscow State University, Moscow 119992, Russia

Abstract

Bursts of the count rate of extensive air showers (EAS) lead to the appearance of clusters in time series that represent EAS arrival times. We apply methods of nonlinear time series analysis to 20 EAS cluster events found in the data set obtained with the EAS-1000 prototype array. In particular, we use the Grassberger–Procaccia algorithm to compute the correlation dimension of the time series in the vicinity of the clusters. We find that four cluster events produce signs of chaotic dynamics in the corresponding time series. By applying a number of supplementary methods we assess that the nature of the observed phenomenon may indeed be chaotic and thus deterministic. We suggest a simple qualitative model that might explain an origin of EAS clusters in general and “possibly chaotic” clusters in particular. Finally, we compare our conclusions with the results of similar investigations performed by the EAS-TOP and LAAS groups.

Key words: Extensive air showers, arrival times, chaotic dynamics
PACS: 96.40Pq, 05.45.A

1 Introduction

We have already studied the distribution of arrival times of extensive air showers (EAS) registered with the EAS-1000 prototype array both by methods of classical statistics [1,2] and by methods of cluster analysis [3,4]. In particular, we presented 20 EAS cluster events—groups of consecutive showers that were

^{*} Corresponding author.

Email addresses: fomin@eas.sinp.msu.ru (Yu.A. Fomin),
 kulikov@eas.sinp.msu.ru (G.V. Kulikov), zotov@eas.sinp.msu.ru
 (M.Yu. Zotov).

registered in time intervals much shorter than expected ones. These groups represent bursts of the EAS count rate and may be considered as cosmic ray bursts, see [3,4]. This phenomenon has put forward at least two questions: one on the astrophysical nature of the process, another on its statistical properties. Namely, while the vast majority of sufficiently long samples satisfy the hypothesis for an exponential distribution of time delays between EAS arrival times [1,2], the χ^2 -test performed for samples taken in the vicinity of some of the EAS clusters made us reject this hypothesis. Thus we have decided to apply methods of nonlinear time series analysis to samples that contain EAS clusters in order to clarify dynamical reasons of this situation. This approach has already proved to be a powerful tool of investigation in different fields of science including different fields of astrophysics in general [5] and cosmic ray physics in particular, see [6,7,8,9,10,11] and references therein.

Recall that the data set under consideration represents 203 days of regular operation of the array for the period August 30, 1997 to February 1, 1999. The total EAS number in the data set equals 1 668 489. The mean number of charged particles in a shower is of the order of 1.2×10^5 . This corresponds to the energy of a primary particle ~ 1 PeV/nucleon. The mean interval between consecutive EAS arrival times is equal to 10.5 s. The discreteness in the moments of EAS registration approximately equals 0.055 s (one tic of the PC clock).

In [12], we have already discussed briefly the results of nonlinear analysis of one of the EAS clusters. In the present paper, we study this cluster in depth and briefly discuss three other clusters that demonstrate nonlinear features.

2 Preliminary Facts

In what follows, we study a scalar time series of the form x_1, x_2, \dots, x_n , where $x_i = t_i - t_{i-1}$, t_i is the moment of registration of the i th EAS, $i = 1, \dots, n$, and $t_0 = 0$ corresponds to midnight. For the purposes of our investigation, it is convenient to use time intervals x_i given in seconds.

One can point out two main approaches to nonlinear analysis of the time series: (1) the scaling exponent and fractal length estimates based on the self-similarity properties of experimental signals [13]; (2) an estimate of the correlation dimension based on the embedding of the original time series in an m -dimensional phase space [14,15,16] (see, e.g., [17] for a comprehensive review). In the current research, we follow the second approach. Within it, the main tool to analyse the dynamics of the time series is the Grassberger–Procaccia method [18] with the modification suggested by Theiler [19]. Namely, given a sample (x_1, x_2, \dots, x_N) extracted from the time series we construct m -

dimensional delay vectors

$$\mathbf{x}_i = (x_i, x_{i+\tau}, x_{i+2\tau}, \dots, x_{i+(m-1)\tau}),$$

where τ is an arbitrary but fixed time increment and m is an embedding dimension. Then we compute the number $K(\rho)$ of vectors with mutual distance less or equal than ρ and such that delay vectors \mathbf{x}_i are shifted by at least W indices:

$$K(\rho) = \sum_{i=1}^{M-W} \sum_{j=i+W}^M \Theta(\rho - \|\mathbf{x}_i - \mathbf{x}_j\|), \quad (1)$$

where Θ is the Heaviside step function, $M = N - (m-1)\tau$, and $W \geq 1$ is the cut-off parameter (the Theiler window). Finally, we plot $\log K(\rho)$ vs. $\log \rho$. For small ρ , the slope of this plot is an estimate of the correlation dimension D_2 :

$$D_2(\rho) = \frac{d \log C_2(\rho)}{d \log \rho},$$

where C_2 is the correlation sum:

$$C_2(\rho) = \frac{2K(\rho)}{(M-W)(M-W+1)}.$$

(Obviously, one may use K instead of C_2 in the expression for the correlation dimension.) A plateau observed in the $D_2(\rho)$ -plot for small ρ or, equivalently, a so called scaling region in the $\log K$ vs. $\log \rho$ plot are regarded as signs of chaotic dynamics in the corresponding time series. A value of D_2 at the plateau is taken as an estimate of the correlation dimension of the attractor underlying the data. This quantity also gives a (lower) estimate for the number of degrees of freedom in the process under consideration.

To compute K , we normally divide each unit interval in $\lg \rho$ into 50 subintervals of equal length. We have found that though this number of subintervals seems to be small, it adequately reflects the qualitative structure of D_2 while a much bigger number of subintervals (≥ 200) leads to considerable fluctuations in D_2 ; these fluctuations hide the structure of D_2 , especially for m large enough. A smaller number of intervals gives too rough structure of D_2 . The derivative is calculated via a standard three-points algorithm. No smoothing or fitting procedures are used.

Notice that Eq. (1) contains four free parameters: N , τ , W , and m . At the preliminary stage of the investigation, we “scanned” the experimental data set having split it into adjacent samples with $N = 128, 256, 512$, and 1024 .

At this step, we used $\tau = 1$, $W = 1$, and odd values of m in the range from 5 to 13. The value of N was chosen to be a power of 2 because this allows one to use fast algorithms of calculating the Fourier transform that is the main part of traditional Fourier analysis. After we had found a number of samples that demonstrated some kind of plateau in the plot of $D_2(\rho)$, we studied the corresponding data with different N in the above range and different values of τ in the range 1–10. (Evidently, in our case τ may take only integer values.) For N large enough, we have performed calculations for m up to 25. In any case, m and τ were chosen such that the number of delay vectors was greater than 100. Finally, to avoid autocorrelation in the time series, we employed $W = 1 \dots 20$.

To compute mutual distances between delay vectors (see Eq. (1)), we tried several norms: the maximum norm L_∞ , the taxicab norm L_1 , and the Euclidian norm L_2 . Recall that for a given m -dimensional vector \mathbf{x} these norms are defined in the following way:

$$\|\mathbf{x}\|_\infty = \sup_{1 \leq i \leq m} |x_i|, \quad \|\mathbf{x}\|_1 = \sum_{i=1}^m |x_i|, \quad \|\mathbf{x}\|_2 = \sqrt{\sum_{i=1}^m |x_i|^2}.$$

Besides these, we have also employed the “dimension scaled” norms L_{1C} and L_{2C} that are expected to provide more reliable results than their classical counterparts [20,21]:

$$\|\mathbf{x}\|_{1C} = \frac{1}{m} \|\mathbf{x}\|_1, \quad \|\mathbf{x}\|_{2C} = \frac{1}{\sqrt{m}} \|\mathbf{x}\|_2.$$

Since the process of calculating D_2 is very time consuming, we have used only one of these norms, namely the maximum norm, to analyse the complete data set. Four other norms were tested for a number of samples both with and without a plateau in the $D_2(\rho)$ -plot obtained with L_∞ .

There are a number of tools that can help one to verify the results of calculating the correlation dimension D_2 , see, e.g., [17]. Among them, we have chosen the Theiler–Takens “maximum likelihood” estimator of the correlation dimension [22,23]:

$$t_{\text{TT}}(\rho) = C_2(\rho) \left[\int_0^\rho \frac{C_2(\rho')}{\rho'} d\rho' \right]^{-1}. \quad (2)$$

This quantity not only provides an efficient means to find out an optimal estimate of the correlation dimension out of the correlation integral but also provides an estimate of the statistical error.

Another problem in the case when a plateau in a plot of $D_2(\rho)$ is observed is to make an assessment about the nature of the dynamics. The main difficulty is to figure out whether one witnesses chaotic dynamics in a deterministic process or a special class of stochastic processes [24,25]. One of the main tools to solve this problem is the method of surrogate data [26,27], see also [28] and references therein. The main idea of this approach is to generate a sufficient number of artificial (“surrogate”) samples that have the same statistical distribution (and possibly some other features) as the experimental data and to study the behaviour of the correlation dimension. If surrogate data demonstrate a plateau in plots of $D_2(\rho)$ then one concludes that the original data is stochastic; otherwise they are likely to be deterministic and chaotic.

Among other tools one can find the quantity

$$t_{\text{BDS}}(m, \rho) = \frac{C_2(m, \rho)}{C_2(1, \rho)^m} \quad (3)$$

suggested in [29] and in the above form—in [30]. As it was shown in [29], for a sequence of independent random numbers, $C_2(m, \rho) = C_2(1, \rho)^m$ holds, where m is the embedding dimension, and thus $t_{\text{BDS}}(m, \rho) \equiv 1$. Therefore, if one finds $t_{\text{BDS}}(m, \rho) \neq 1$ for ρ where a plateau in the $D_2(\rho)$ -plots is observed then one may conclude that the nature of the dynamics is chaotic.

Besides this, we used a function suggested in [31]:

$$\phi_0(\rho) = \frac{D_2(m_2, \rho) - D_2(m_1, \rho)}{m_2 - m_1}, \quad (4)$$

where m_1 and m_2 are different embedding dimensions. For independent random data, $\phi_0(\rho) \neq 0$ and $\phi_0 \rightarrow 1$ as $\rho \rightarrow 0$. We also employed the “normalized slope” introduced in [21]:

$$\phi(m, \rho) = \frac{1}{m} D_2(m, \rho). \quad (5)$$

If $\phi(m, \rho)$ does not converge to 0 in a wide range of ρ as m grows but to some value ≥ 0.1 , then most probably data do not represent a chaotic process but should be treated by statistical techniques [21].

Recall that before applying nonlinear techniques to the analysis of a time series, it is strongly suggested to check whether the time series is really nonlinear. In particular, one can try a measure for time-reversibility, which is considered

to be a good indicator for nonlinearity [32]. For the data sorted in time order,

$$\gamma = \frac{1}{(\sigma^2)^{\frac{3}{2}}(N-1)} \sum_{i=2}^N \left(\frac{x_i - x_{i-1}}{s_i - s_{i-1}} \right)^3 \quad (6)$$

is calculated, which is just the mean of the slopes, taken to the third power; here s_i are the moments of time and σ^2 is the variance of the sample. (In our case, $s_i - s_{i-1} = 1$ since x_i represent just numerated time delays.) For a time series generated by a linear process and for the surrogate data, one expects $\gamma \approx 0$. In contrast, time series with nonlinearities can be asymmetrical in time and may yield values of $\gamma \neq 0$. To check, whether γ significantly deviates from zero for the studied sample, one should generate a sufficient number of surrogate data. To pay regard to deviations in both directions ($\gamma > 0$ and $\gamma < 0$), a two sided test has to be performed [26].

Finally, a few words are in order about stationarity of the time series under consideration. As is well known, a fundamental assumption underlying almost all existing linear and nonlinear techniques of time series analysis is that the time series is stationary, see, e.g., [33]. As we have already mentioned earlier [2,4,34], the count rate of EAS depends on the value of the atmospheric pressure. For the data obtained with the EAS-1000 prototype array, this dependence can be approximately expressed by a simple formula

$$\ln N_{\text{EAS}} = -\beta P + \text{const},$$

where N_{EAS} is the number of EAS registered in a time unit, P is the atmospheric pressure, mm Hg, and $\beta \approx 10^{-2}$ is the barometric coefficient. This effect makes the time series non-stationary. To provide stationarity (at large time scales) we adjusted time delays between consecutive showers to the atmospheric pressure $P^* = 742$ mm Hg which is close to the average pressure for the whole analyzed data set. This adjustment was made by the following formula:

$$x_i = x_i^0 \exp[\beta(P^* - P_i)],$$

where x_i^0 is the experimental time delay, and P_i is the atmospheric pressure at the i th delay. The barometric coefficient was chosen to be $\beta = 1.08 \cdot 10^{-2}$, exactly as in our previous paper [4]. Due to the adjustment, the mean and the variance of the time series at large time scales were approximately constant.

Remark 1 *In fact, since we shall discuss only comparatively short samples, the above adjustment to P^* is not important for the present results because atmospheric pressure does not change significantly during periods of time covered*

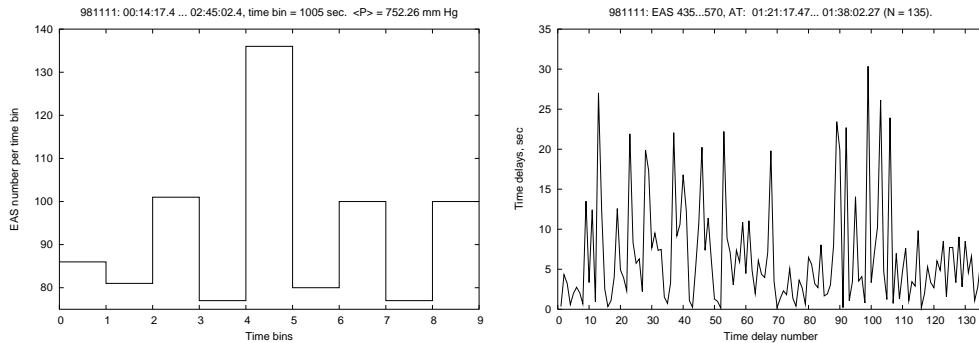


Fig. 1. The count rate at a time interval that contains the cluster registered on November 11, 1998 (left); the cluster is presented by the central bin. Time delays (s) between EAS that constitute the cluster (right). The delays are adjusted to $P^* = 742$ mm Hg.

by the samples. We perform the adjustment in order to guarantee stationarity of the whole time series.

To compute the correlation sum C_2 effectively, we have worked out an algorithm based on preliminary sorting of mutual distances between delay vectors. Though quite simple, the algorithm occurred to be up to 10 times faster than a straightforward computation of C_2 . To perform calculations, we employed GNU Octave [35] running in Mandrake Linux.

3 The Main Results

As is well known, one needs sufficiently long samples to perform a successful time series analysis. On the other hand, the bursts of the EAS count rate have comparatively short time range. Thus we did not in fact expect to find signs of chaotic dynamics in the vicinity of EAS clusters. Surprisingly, we have found some.

Having “scanned” the available data set, we found that for the overwhelming majority of data samples no scaling region is observed in $\log C_2$ vs. $\log \rho$ plots. This is quite natural since arrival times of extensive air showers represent a simple stochastic process such that for sufficiently long samples, the number of EAS registered in a time unit obeys the Poisson distribution in a wide range of time delays, see, e.g., [2]. Still, we have come across a number of samples with a plateau in the $D_2(\rho)$ -plot in the vicinity of four EAS clusters, namely those registered on May 14, November 11, and December 28, 1998 and on January 8, 1999. Let us begin our discussion with the second of these events, which is the longest one.

The cluster event observed on November 11, 1998 consists of 136 EAS regis-

tered within the period from 01:21:17.47 to 01:38:02.27 (Moscow local time, MSK¹) with the atmospheric pressure $P = 752.3$ mm Hg, see Fig. 1. Within the whole data set obtained on November 11, 1998 the showers that form the cluster event have numbers 435–570. The event is made up of three clusters, which begin at consecutive arrival times (i.e., the first cluster begins at the shower #435, the second one begins at the shower #436, etc.) and end up simultaneously at the shower #570. In our opinion, the appearance of three clusters does not reflect any process of astrophysical nature but is caused by the technique of their selection (see [4] for the details). Thus we treat the event as a single (outer) cluster. The real duration of this cluster equals 1004.8 s while the adjusted duration equals 898.8 s; the probability of the appearance of such a cluster is of the order of 2×10^{-7} .

Let us take a look at a number of samples in the vicinity of the cluster in order to see how the correlation dimension D_2 changes when the cluster appears. To make this influence more clear we shall not only present samples with a plateau in the plot of $D_2(\rho)$ but also a typical sample outside the cluster. Besides nonlinear tools, we shall employ the classical Fourier analysis. Recall that it is suggested for the Fourier analysis to have $x(1) \approx x(N)$. All samples discussed below are chosen to satisfy this demand. In particular, we omit the last shower of the cluster and consider a sample that consists of 134 instead of 135 delays. Obviously, this does not influence D_2 and other quantities significantly.

Figure 2 shows the correlation dimension (the left column) and the power spectrum density (PSD) (the right one) calculated for three samples in the vicinity of the cluster. The top row represents a sample that consists of EAS #435–569 and thus contains the cluster without the last delay. The length of the sample $N = 134$. The middle row represent a sample that contains the cluster but consists of $N = 256$ delays (EAS #425–681). The bottom row represents a sample that immediately follows the second one. It also consists of 256 delays (EAS #682–938). The correlation dimension was computed for $\tau = 1$, $W = 1$, and $m = 1, \dots, 12$.

What can be seen from this figure? In our opinion, the most important thing is that one can see plateaus in both plots of $D_2(\rho)$ that represent samples with the cluster. To the contrary, no plateau is observed for the sample outside the cluster. We stress that in this sense, the sample is typical for the whole data set.

Next, it is remarkable that the influence of the cluster on the behaviour of the correlation is not restricted to the cluster itself, e.g., the sample made of EAS #425–681 begins approximately 2.5 min before the cluster and ends up in 23.5 min after it. Our analysis has revealed that a plateau can be observed

¹ Recall that MSK is connected to UT as follows: $T_{\text{MSK}} = T_{\text{UT}} + 3 + \Delta$ (hours), where $\Delta = 1$ during Daylight Saving Time, 0 otherwise.

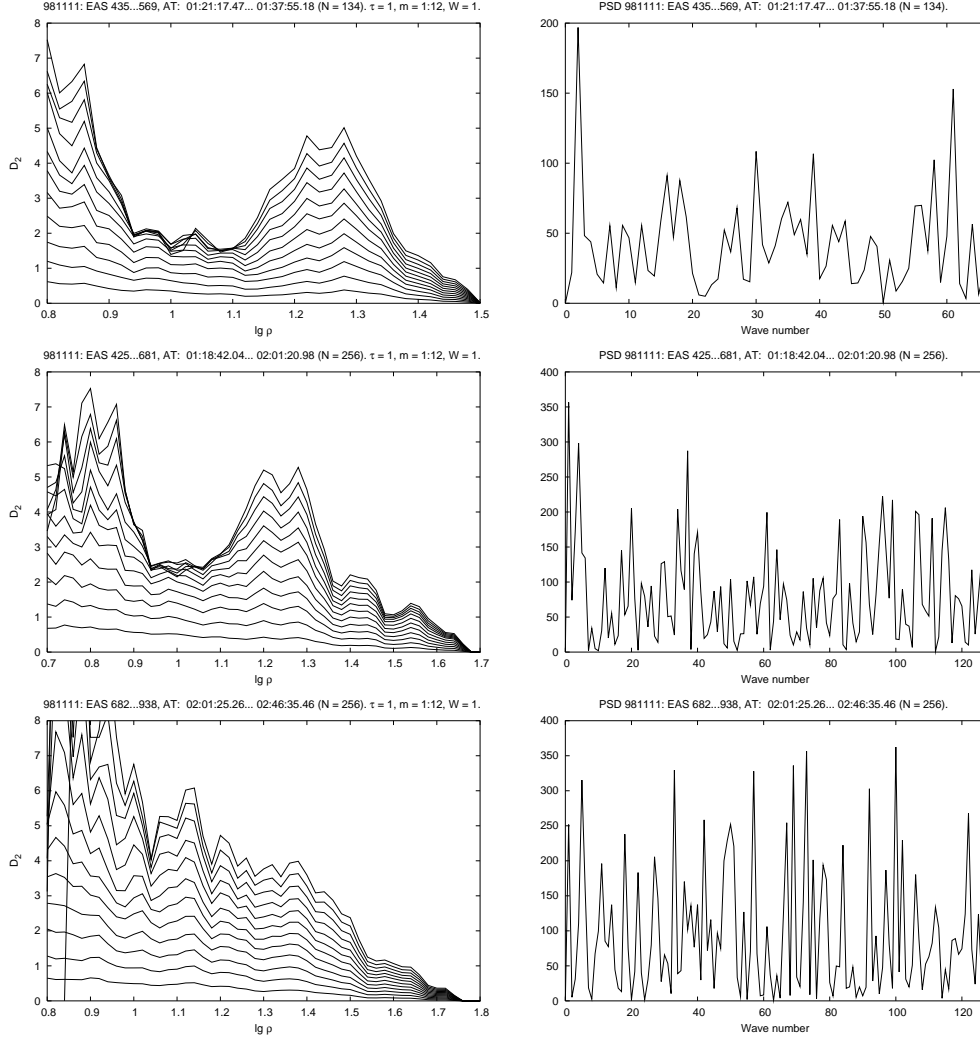


Fig. 2. The correlation dimension $D_2(\rho)$ (the left column) and the power spectrum density (the right column) for a number of samples in the vicinity of the cluster registered on November 11, 1998. From top to bottom: a sample with the cluster (without the last delay), EAS #435–569, $N = 134$; a sample that contains the cluster as a subset, EAS #425–681, $N = 256$; a sample that follows the second one, EAS #682–938, $N = 256$. The distance ρ is given in seconds.

even for samples with $N \sim 500$ lying in the range of EAS numbers 340–1000. It is also interesting to mention that the plateau is more pronounced if a sample contains more of the after-cluster showers than those arrived before.

The level of the plateau changes for different N . The correlation dimension fluctuates around $D_2 \approx 1.77$ for the sample with $N = 134$ while $D_2 \approx 2.45$ for the sample with $N = 256$. This may be due to low numerosness of the samples and/or white noise effects.² Notice that for both samples with a plateau the demand $m > 2D_2 + 1$ is satisfied if we assume that D_2 is given

² We thank an anonymous referee for pointing this out to us.

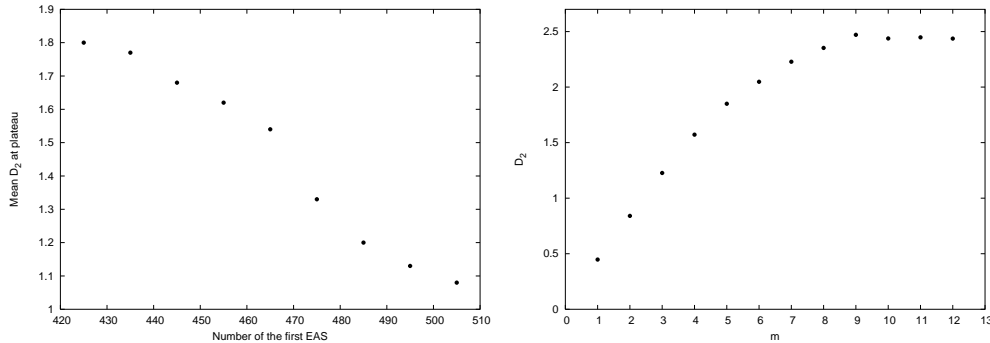


Fig. 3. The left panel: dependence of the correlation dimension $D_2(\rho)$ on the position of the sample ($N = 134$). The right panel: dependence of the correlation dimension at the plateau on the value of the embedding dimension (EAS #425–681, $N = 256$).

by the level of the corresponding plateau (see, e.g., [36]). We also remark here that the level of a plateau varies for samples with the same length but with different positions with respect to the cluster. The left panel in Fig. 3 shows the dependence of the mean value of D_2 at a plateau on the position of a sample. All samples have the same length $N = 134$ but begin at different EAS from #425 up to #505. EAS #425 arrived at 01:18:42.04 MSK, EAS #505 arrived at 01:30:42.15, thus the left ends of these samples cover 12-minute time interval. It is evident from the plot that the value of the correlation dimension takes different values and monotonically decreases from ≈ 1.80 to ≈ 1.08 . For samples that begin at $\text{EAS} \geq 510$ a plateau becomes shorter and soon disappears.

The right panel in Fig. 3 demonstrates how the value of D_2 saturates as the embedding dimension m grows. The plot is made for the sample that consists of EAS #425–681. It is clearly seen that the saturation takes place at $m = 9$ but not at $m = 3$ as one may expect for this value of D_2 and a purely chaotic time series. As it was shown in [37], this may be due to the presence of observational noise and small length of the sample. The demand $N \geq 10^{D_2/2}$ [38] is also obviously hold.

Finally, one can notice that the plateaus are not as “smooth” and long as one may like to see. In this connection, we would like to mention two things: (1) Experimental data are affected by noise that can spoil the picture; we plan to employ special noise filtering techniques in future. (2) We do not use any smoothing techniques while calculating D_2 . They can improve a plot of D_2 but the situation remains qualitatively the same.

Now let us turn to the right column of Fig. 2. This column presents the results of the Fourier analysis of the three samples. The PSD of the sample without a plateau is a broadband one, which is typical for a random noise signal. The PSDs of two other samples do not also differ significantly from a broadband one. Still it seems worth mentioning that for both samples with a plateau one

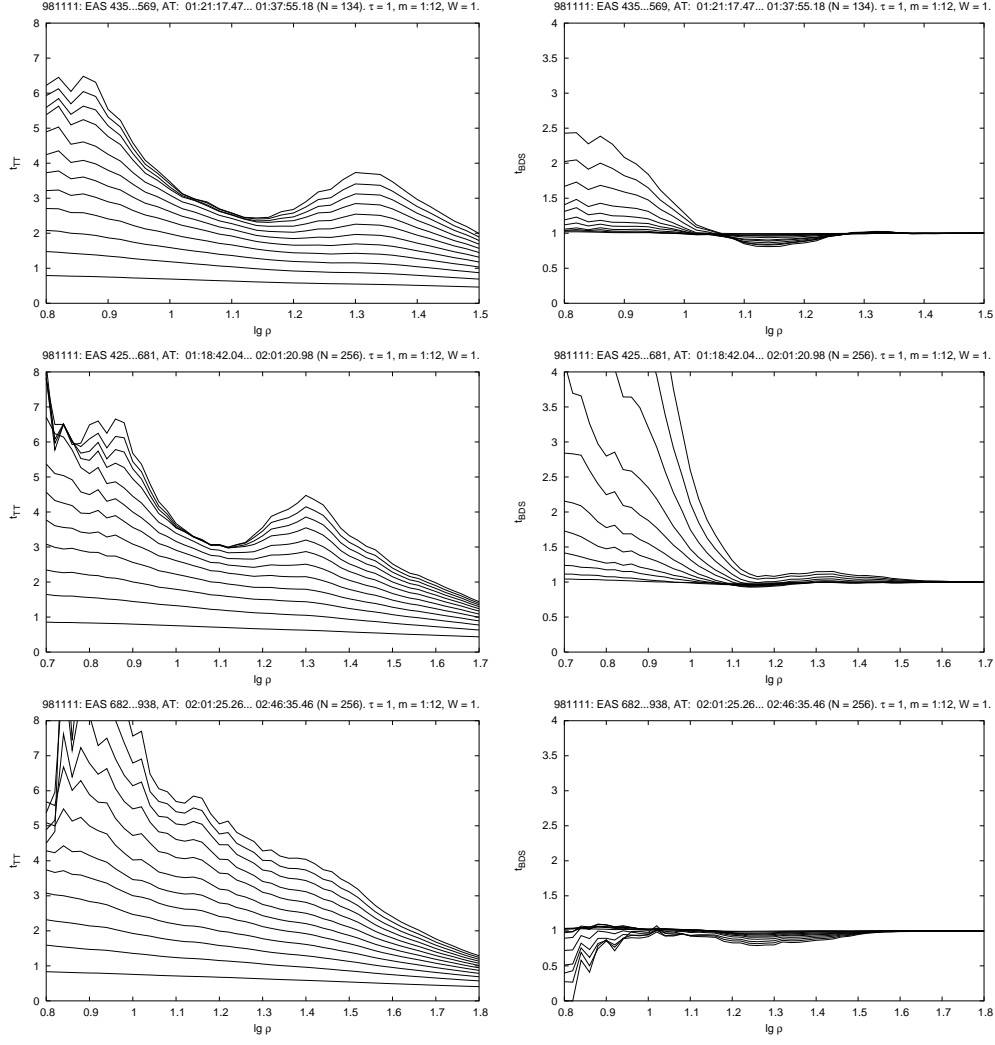


Fig. 4. The left column: the Theiler–Takens estimator, see Eq. (2). The right column: t_{BDS} , Eq. (3). The functions are computed for the same samples and values of τ , W , and m as in Fig. 2.

can see the highest peaks located at the left end of the spectrum. This is true for almost all samples with a plateau in D_2 -plots we have found.

Next, let us employ the tools discussed in Section 2 in order to obtain a deeper insight in the observed phenomenon. For brevity, let us call the samples with a plateau in D_2 -plots ‘possibly chaotic’ (PC). Our aim is to figure out whether they are indeed chaotic or represent a special stochastic process.

As one can see from Fig. 4, the Theiler–Takens estimator (2) does not have a clear plateau for either samples but the behaviour of t_{TT} for the PC samples noticeably differs from that for the third one. Namely, for the PC samples the t_{TT} -curves saturate for the corresponding intervals of $\lg \rho$ for $m > 8$ while for

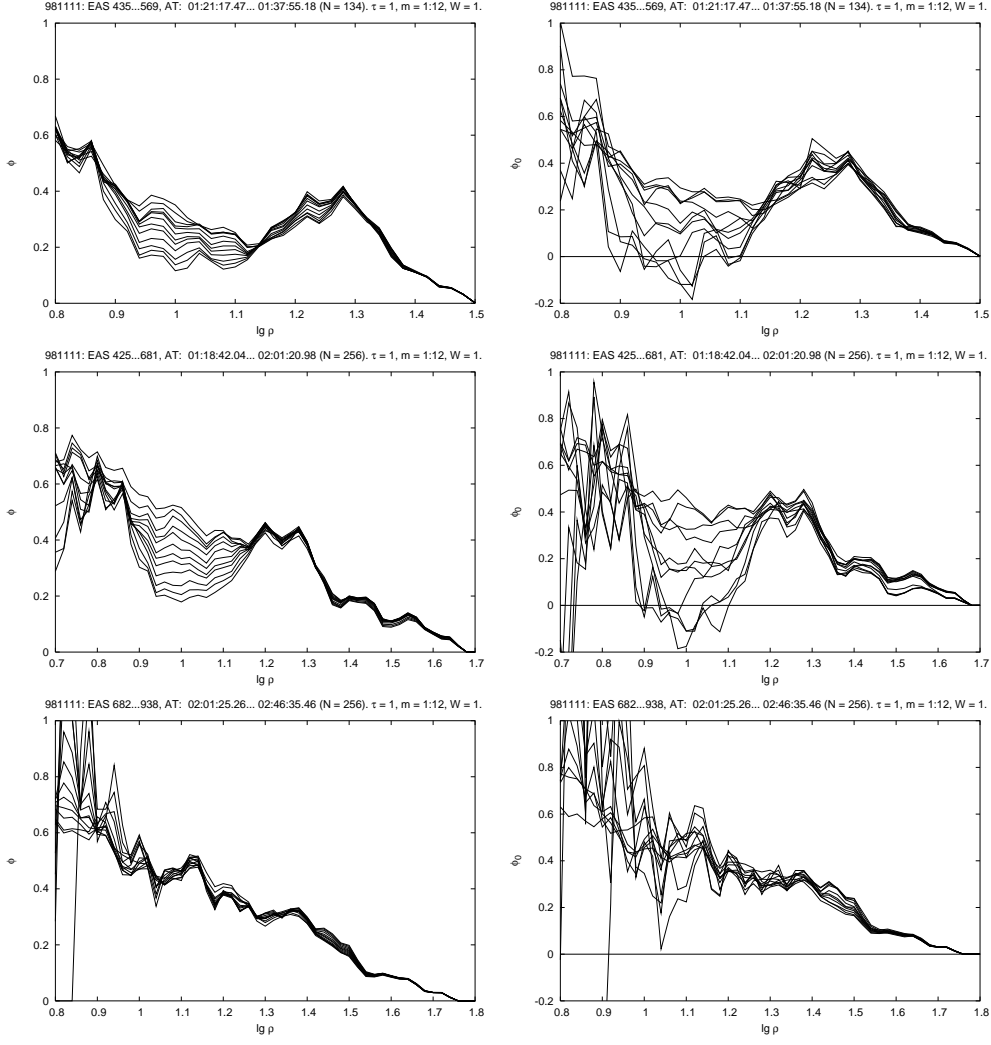


Fig. 5. The left column: the normalized slope ϕ , see Eq. (5). The right column: the function ϕ_0 given by Eq. (4), $m_2 - m_1 = 1$. The functions are computed for the same samples and values of τ , W , and m as in Fig. 2.

the third sample the curves stay separated.³

Next, the right column of Fig. 4 depicts the behaviour of t_{BDS} , see Eq. (3). One can see that for both PC samples and m big enough, t_{BDS} noticeably differs from 1 at the intervals where plateaus of the correlation dimension are observed [$\lg \rho \in (0.94, 1.12)$ for the first sample and $\lg \rho \in (0.94, 1.08)$ for the second one]. Conversely, $t_{\text{BDS}} \approx 1$ for $\lg \rho \geq 0.94$ for the third sample. As it follows from the properties of t_{BDS} discussed above, this kind of behaviour witnesses in favour of a chaotic nature of the PC samples and a stochastic nature of the sample without a plateau in the D_2 -plot.

³ We would like to mention that one can find samples such that sufficiently clear plateaus can be observed for both D_2 - and t_{TT} -plots, see the first version of this paper for the details [39].

Fig. 5 depicts the normalized slope ϕ (see Eq. (5)) and the function ϕ_0 (Eq. (4)) for the same three samples. One can see that the behaviour of these functions for the PC samples noticeably differs from that for the third one. Still, the situation is not unequivocal. Namely, for both PC samples, ϕ_0 fluctuates around zero at the corresponding intervals of $\lg \rho$ thus giving an argument in favour of a chaotic nature of these samples. On the other hand, the limiting values of the normalized slope ϕ (the bottom curves) lie above 0.1 at the same intervals of $\lg \rho$ thus suggesting a stochastic nature of the samples. This controversy can probably be resolved if we recall that ϕ converges slowly, see [21]. Really, the level of the “hollows” in the plots of ϕ decreases if we increase m reaching the values ≈ 0.1 and ≈ 0.15 for the first and the second PC samples respectively and $m = 15$. For $m > 15$ the number K of close delay vectors at the corresponding intervals becomes ≤ 100 thus not providing a value statistically necessary for accurate computation of the correlation dimension.

Next, let us say a few words about the results of surrogate data tests. For the first PC sample, we generated 99 “shuffled” surrogates obtained by a random permutation of time intervals x_i in a given sample. This number of surrogates corresponds to a 98% level of significance (L.S.) of the statistical test [32]. For the second sample, we made 39 “shuffled” surrogates (95% L.S.) and 39 surrogates based on the amplitude adjusted Fourier transform method proposed in [27]. To obtain these surrogates, we employed the TISEAN package [40]. None of these “Fourier-based” surrogates demonstrated a plateau in D_2 -plots thus revealing that the consequence of time delays that constitute the original data is crucial for the appearance of plateaus. Therefore, the results of this test suggest that the PC samples represent a chaotic (and thus nonlinear) process.

On the other hand, the test for time-reversibility based on γ -statistic (6) did not detect nonlinearity in the PC samples. Namely, for the first PC sample $\gamma = 0.74$ while $\gamma \in (-1.38, 1.28)$ for the surrogates. For the second PC sample, $\gamma = -0.22$ while surrogates gave $\gamma \in (-0.44, 0.45)$. (To compare, $\gamma = -0.38$ for the third sample.) These results imply that the hypothesis for time-reversibility of the PC samples cannot be rejected. Therefore, these samples may be linear (or obtained by a transformation of a linear process) thus excluding the possibility of chaotic dynamics.

Thus, it is interesting to figure out what kind of stochastic processes can describe the distribution of time delays in the PC samples. To do this, we performed the χ^2 -test to verify the hypothesis that time delays between consecutive arrival times have an exponential distribution. We used different time bins in the range from 1 to 10 s with a step equal to 0.5 s providing that each bin taken into account contains more than 10 events. We have found that for both PC samples, this hypothesis should be rejected with at least 90% L.S. while for the third sample the hypothesis may be accepted with 85% L.S.

In addition, we remark that for the above PC samples a plateau was only found for $\tau = 1$ and the maximum norm. Still there are PC samples in the vicinity of the cluster that demonstrate a plateau in the D_2 -plots for $\tau = 2$ and both “dimension scaled” norms, see [39] for the details. For all PC samples, a plateau is observed in a wide range of the Theiler window W (up to 20).

Now let us briefly discuss three other EAS clusters that produce signs of chaotic behaviour in the corresponding time series. Table 1 contains certain information about these clusters as well as the cluster discussed above. Notice that while the cluster registered on January 8, 1999 is sufficiently long ($N_{\text{EAS}} = 134$) two other clusters are short and this makes an appearance of signs of chaos in much longer samples very surprising. It is also worth mentioning that the fourth cluster (December 28, 1998) was registered within the period of observation of the GRB No. 7285 in the BATSE Catalogs [41].

Table 1
EAS clusters that produce signs of chaotic dynamics

Date dd.mm.yy	Beginning hh:mm:ss	End hh:mm:ss	EAS Numbers	N_{EAS}	\mathcal{P}_{adj}
11.11.98	01:21:17.47	01:38:02.27	435–570	136	2×10^{-7}
08.01.99	00:19:47.03	00:32:26.31	145–278	134	4×10^{-7}
14.05.98	22:24:50.09	22:24:54.70	7567–7574	8	2×10^{-8}
28.12.98	15:22:33.18	15:23:17.34	5695–5712	18	5×10^{-7}

Notation: N_{EAS} —the number of EAS in a cluster; \mathcal{P}_{adj} —the probability of an appearance of the cluster assuming that time delays between consecutive EAS are adjusted to the pressure $P^* = 742$ mm Hg and the distribution of the number of EAS registered in a time unit (for the whole data set) obeys the Poisson distribution with the intensity $\lambda \approx 5.77 \text{ min}^{-1}$. Moscow local time is given.

Table 2 presents the results of calculation of the correlation dimension for a number of samples in the vicinity of the clusters as well as the results of a number of tests discussed above. For the last three samples, the given values of \bar{D}_2 were computed for $m = 15, 17$, and 14 respectively. Notice that the PC sample for January 8, 1999 is shifted with respect to the cluster. The cluster by itself does not produce signs of chaotic dynamics. For this event, a plateau can be observed not only for $\tau = 1$ but also for $\tau = 2$ and 3 . For the cluster registered on May 14, 1998, a plateau can also be observed for $\tau = 2$. For the last cluster, a plateau was observed only for $\tau = 1$. To the contrary to most other PC samples, a plateau exists not only for the maximum norm L_∞ but also for the norms L_2 and L_{2C} . For all PC samples, a plateau was found in a wide range of values of the Theiler window W . This means that autocorrelation, which can lead to spurious results, is avoided.

Table 2

Results of different tests applied to PC samples

Date dd.mm.yy	PC EAS Numbers	\bar{D}_2	max ΔD_2	t_{BDS}	ϕ	ϕ_0	SDT	γ -test	χ^2 -test
11.11.98	435–569	1.77	0.11	\pm	–	+	+	–	–
	425–681	2.45	0.12	\pm	–	+	+	–	–
08.01.99	105–232	0.74	0.03	+	+	+	+	–	+
14.05.98	7499–7627	1.40	0.04	\pm	+	+	+	–	+
28.12.98	5632–5760	1.28	0.07	+	+	+	+	\pm	+

Notation: PC EAS Numbers—the range of EAS numbers for a PC sample (to be compared with the range of EAS that form the corresponding cluster); \bar{D}_2 —the mean value of the correlation dimension at a plateau for a maximum value of m , see the text; $\max \Delta D_2$ —the maximum value of the statistical error of \bar{D}_2 ($\Delta D_2(\rho) = D_2(\rho)/\sqrt{K(\rho)}$). Columns t_{BDS} , ϕ , ϕ_0 , SDT (surrogate data test), and γ -test present results of the corresponding tests: “+” if a test witnesses in favour of a chaotic nature of the sample under consideration, “–” otherwise; “ \pm ” means that no definite conclusion can be made. The last column presents the results of the χ^2 -test of the hypothesis for an exponential distribution of time delays within a sample: “+” means that the hypothesis may be accepted for some choice of time bins, “–” otherwise. For all data, $\tau = 1$, $W = 1$, and the maximum norm is used.

As one can see from Table 2, the results of the tests applied to these three events are mostly similar to those for the first cluster. Namely, none of the surrogate samples (39 “shuffled” and 39 Fourier-based surrogates) demonstrates a plateau in the $D_2(\rho)$ -plot thus implying a chaotic nature of the original samples. On the other hand, the test for time-reversibility usually does not detect nonlinearity in the PC samples. The only exception is the last sample in Table 2. For this sample, the γ -test applied to shuffled surrogates gives the usual result but being applied to Fourier-based surrogates it rejects the hypothesis for time-reversibility with 95% L.S. It is worth mentioning that this result has been confirmed when we employed another technique of making Fourier-based surrogates also implemented in TISEAN. Next, for all PC samples the Theiler–Takens estimator t_{TT} demonstrates either a plateau or an interval where the curves saturate as the embedding dimension m grows. Finally, it is interesting to note that for three PC samples we have found a way of grouping time intervals that allows one to accept a hypothesis for an exponential distribution of time delays within the corresponding PC sample. Still we must remark that for the majority of groupings this hypothesis should be rejected with at least 90% L.S.

Thus we come to a conclusion that the observed dynamics of time intervals between consecutive EAS in the vicinity of these four clusters may indeed be

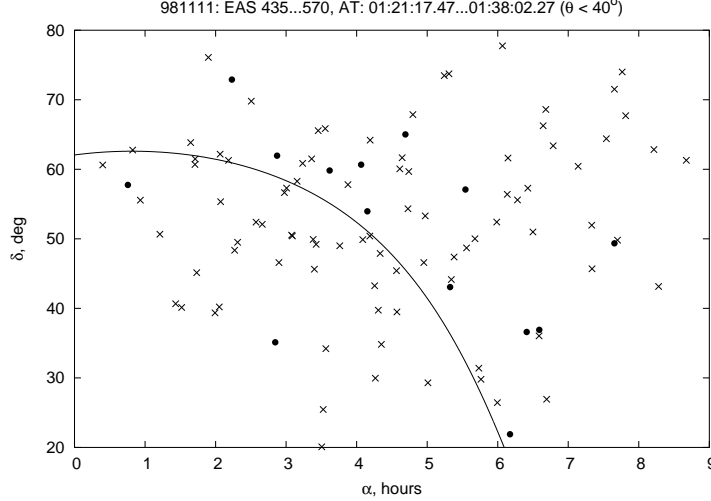


Fig. 6. Arrival directions (AD) of EAS that form the cluster registered on November 11, 1998 and have zenith angle $\theta < 40^\circ$: \bullet —AD of EAS with $N_e \geq 9.7 \times 10^4$, \times —AD of all other EAS. The curve shows the Galactic plane. Equatorial coordinates are used.

chaotic though this cannot be assessed unequivocally at the moment. Further investigation is necessary.

4 Discussion

To get a deeper insight into physics of EAS clusters, let us consider the cluster registered on Nov. 11, 1998 from another point of view. A natural question that arises when one finds a burst of EAS count rate is whether primary particles that led to the appearance of the burst had had a common compact source. Fig. 6 shows arrival directions of EAS that belong to the cluster and have zenith angle $\theta < 40^\circ$. Obviously, one cannot give a positive answer to the above question. Still, this seems quite natural since the energy of primary particles in our case is too low to “remember” the source. Besides this, the majority of EAS in the cluster represent a normal count rate. Namely, since we register 5.7 EAS/min in average and the duration of the cluster adjusted to $P^* = 742$ mm Hg equals approximately 15 min then we may expect to register 85–86 EAS within this period. Naturally, arrival directions of these EAS should be distributed more or less isotropically. Thus, one may expect to observe a kind of a cluster in arrival directions for only remaining 50 EAS. Still, this does not happen. One can see doublets and triplets of showers with almost coincident arrival directions and a kind of grouping along the Galactic plane but no big groups of EAS are observed.

Another question is whether clusters consist of EAS that are more “powerful”

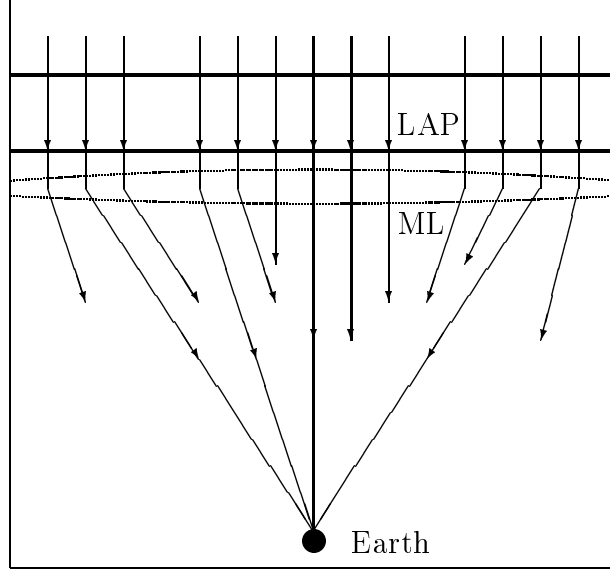


Fig. 7. Model of EAS clusters appearance. Notation: LAP—a layer of accelerated particles; ML—magnetic lens.

than the others. Surprisingly enough, but the answer is negative. As we have already mentioned in Section 1, the mean value of electrons \bar{N}_e^{tot} in EAS in our data set is of the order of 1.2×10^5 particles. To compare, for the above cluster $\bar{N}_e \sim 9.7 \times 10^4$, and only 14 EAS have $N_e > \bar{N}_e$, see Fig. 6. Two of these EAS have $N_e \sim 10^6$. On the other hand, at least 41 EAS have $N_e < 1/2 \bar{N}_e$. (We remark that the geometry of the EAS-1000 prototype array does not allow one to obtain parameters of all registered EAS.)

A similar situation is observed for other EAS clusters, both PC and “ordinary” ones. Thus, we come to the following observations: (i) EAS in a cluster do not have a joint source (arrival direction); (ii) the majority of EAS in a cluster have $N_e < \bar{N}_e^{\text{tot}}$. This allows us to suggest a simple conceptual model that is intended to explain qualitatively how EAS clusters might be produced. To do this, we need only to assume that a considerable part of EAS that constitute clusters are generated by charged particles.

As is well known, the interstellar space is filled with strong and highly inhomogeneous magnetic fields. Still, average magnetic fields in the heliosphere are not strong enough to influence the dynamics of particles with $E \gtrsim 10$ TeV/nucleon (see, e.g., [42]). On the other hand, a series of long-term investigations based on data obtained with Voyager 1, 2, and other space crafts have demonstrated that the large-scale magnetic field strength fluctuations frequently have large amplitudes and are intermittent, and that regions of relatively intense magnetic fields can have a radial extent of more than 10 AU, see [43] and references therein.

Basing on these results, let us consider the following situation. Suppose there is an extended and sufficiently “thick” layer of accelerated particles (LAP) (possibly called a “wave”) that moves through space towards Earth, see Fig. 7. Normally, if it just passes through, an EAS array registers only a few particles originated from the LAP. Now suppose that the LAP meets a region of an extended strong and inhomogeneous magnetic field that works as a lens. If it happens that this “magnetic lens” declines particles in way that they get focused in a “proper” direction then an array may register an excess of EAS over the normal count rate, i.e., an EAS cluster. Notice that from an observer’s point of view showers in the cluster may have very different arrival directions. In our opinion, the fact that the majority of EAS in the observed clusters are less “powerful” than an average shower witnesses in favour of this model since we do not need too strong magnetic fields. The duration of a cluster depends on the thickness of the LAP and the time during which the magnetic lens “works.”

Now let us ask ourselves how does it happen that the time series that represent the majority of EAS clusters (as well as the other data) are stochastic but some clusters seem to demonstrate signs of chaotic dynamics. At the moment, we cannot give a definite answer but can only conjecture that different factors may be involved in this phenomenon. Among them, one can mention a possibly fractal nature of the interstellar medium (see, e.g., [44] and references therein), nonlinear mechanisms of particles acceleration, etc. A very interesting possibility for EAS time series to become chaotic suggests the fact that the large-scale fluctuations in the interplanetary magnetic field strength sometimes have fractal or multifractal structure [45]. This phenomenon has been observed at different distances from Earth and for very different time scales. It is likely that in case that the “magnetic lens” discussed above has certain fractal or multifractal properties then it may lead to the appearance of chaotic dynamics in EAS time series.

Certainly, the presented model is only conceptual and oversimplified. Still we hope that it reflects the nature of processes that may lead to the appearance of EAS clusters, both “ordinary” and “possibly chaotic” ones.

Finally, it is interesting to compare our results with the conclusions of similar investigations performed by other research groups. In a considerable number of articles devoted to the nonlinear time series analysis, one can find a comprehensive investigation of EAS arrival times registered with the EAS-TOP array [6].

Basing on a detailed study of the available experimental data set and the results obtained with the underground muon monitor [7] the authors of this work made a conclusion that cosmic ray signals are all colour random noise, independently of the nature of the secondary particle and of the primary

parent particle, but an existence of deterministic chaotic effects in cosmic ray time series cannot be completely excluded. It was also demonstrated in one of the following articles that an impact of background noise brings additional difficulties to the problem of distinguishing between chaotic and stochastic dynamics [8]. In our opinion, these conclusions as a whole do not contradict our results, especially in view of the fact that signs of chaotic behaviour have only been observed for about 0.1% of EAS in the whole data set.

Besides this, a whole series of investigations devoted to the nonlinear analysis of EAS time series are carried out in Japan beginning from early 1990s at the experimental arrays that now constitute the LAAS network, see, e.g., [10,11] and references therein. The authors of these investigations presented several dozens of events that demonstrate chaotic dynamics. More than this, it was conjectured that the observed dynamics may be due not only to the chaotic structure of the medium through which particles have traversed but also to the nature of the primary particles [46]. Later on, there was suggested a model according to which chaotic events may be generated by cosmic rays that have a structure of a fractal wave arriving from a nonlinear accelerator like a supernova remnant [47]. This model needs to be studied in details, but seems to be promising. Thus that the results obtained during our analysis do not contradict the conclusions of similar investigations performed at other EAS arrays.

The results presented above demonstrate that one can observe an unusual dynamics of EAS arrival times in the vicinity of certain clusters of EAS with the electron number of the order of 10^5 . While the overwhelming majority of samples in our data set are unambiguously stochastic, a number of samples in the vicinity of four EAS clusters demonstrate signs of chaotic dynamics. Still it is rather difficult to make a final conclusion on the nature of this phenomenon: Does it represent deterministic chaos or a special type of a stochastic process? In our opinion, the majority of the tests performed witness in favour of the first of these two alternatives. Nevertheless we must mention that our analysis may somehow suffer of the fact that the phenomena discussed above are only observed at comparatively short time scales with short samples while time series analysis usually prefers longer samples. In this connection, we recall that our investigation of EAS clusters has revealed an existence of “super clusters,” i.e., clusters that have duration more than 30 min and consist of hundreds of EAS. Our future plans include an analysis of these events.

It seems to be necessary to continue the work in this area and to involve some other methods of nonlinear time series analysis. There are a number of other nonlinear tools that may help to make a more definite conclusion about the nature of the observed phenomenon. Among them, one can recall space-time-separation and recurrence plots and the Lyapunov exponents. There are also a number of other measures of nonlinearity besides the one used above [17].

Last but not least, special signal filtering techniques may be used in future to reduce effects of background noise on the dynamics of PC samples.

Finally, as we have already mentioned above, perhaps the biggest puzzle in connection with signs of chaos in EAS time series is their astrophysical nature. It is likely that clusters that produce signs of chaotic dynamics in the corresponding time series are similar to the upper part of an iceberg in a sense that they do not present the complete process but only the most pronounced part of it. We point out that for all PC samples discussed above, the value of the correlation dimension is comparatively small ($D_2 < 3$). Since this value gives a lower estimate for the number of degrees of freedom in the underlying process, it is possible that the structure of this process is not too complicated. Still it seems to be a great challenge to work out a good model that could explain chaotic dynamics in EAS arrival times.

Acknowledgements

We gratefully acknowledge numerous useful discussions with A. V. Igoshin, A. V. Shirokov, and V. P. Sulakov who have helped us a lot with the experimental data set. We also thank Thomas Schreiber for a very helpful communication and anonymous referees for stimulating comments. This work was done with financial support of the Federal Scientific-Technical Program “Research and design in the most important directions of science and techniques” for 2002–2006, contract No. 40.014.1.1.1110, and by Russian Foundation for Basic Research grant No. 02-02-16081.

Only free, open source software was used for this investigation.

References

- [1] O.V. Vedenev et al., *Izv. Ros. Akad. Nauk, Ser. Fiz.* 65 (2001) 1224.
- [2] Yu.A. Fomin et al., *Proc. 27th ICRC, Hamburg, Vol. 1* (2001) p. 195; astro-ph/0201343.
- [3] O.V. Vedenev et al., *Izv. Ros. Akad. Nauk, Ser. Fiz.* 65 (2001) 1674.
- [4] Yu.A. Fomin et al., Clusters of EAS with electron number $\gtrsim 10^4$ (Preprint SINP MSU 2002-9/693); astro-ph/0203478.
- [5] See, e.g., “Chaotic Phenomena in Astrophysics,” eds. J.R. Buchler and H. Eichhorn, *Annals of the N.Y. Academy of Sciences*, v. 497 (1987) and a special issue of *Geophys. Res. Lett.* 18, No. 8 (1991) devoted to the discussion of chaos and stochasticity in space plasmas.

- [6] M. Aglietta et al., J. Geophys. Research 98 (1993) 15241.
- [7] L. Bergamasco et al., J. Geophys. Research 97 (1992) 17153.
- [8] L. Bergamasco et al., J. Geophys. Research 99 (1994) 4235.
- [9] K. Kudela, D. Venkatesan, Nucl. Phys. B (Proc. Suppl.) 39A (1995) 127.
- [10] T. Kitamura et al., Astropart. Phys. 6 (1997) 279.
- [11] S. Saito et al., Proc. 27th ICRC, Hamburg, vol. 1, (2001) p. 212.
- [12] M.Yu. Zotov et al., Izv. Ros. Akad. Nauk, Ser. Fiz. 66 (2002) 1585–1588; astro-ph/0205260.
- [13] B.B. Mandelbrot, The Fractal Geometry of Nature (Freeman, San Francisco, 1982).
- [14] N.H. Packard et al., Phys. Rev. Lett. 45 (1980) 712.
- [15] F. Takens, Lecture Notes in Mathematics, Springer-Verlag, Berlin, vol. 898, (1981) p. 366.
- [16] R. Mañé, Lecture Notes in Mathematics, Springer-Verlag, Berlin, vol. 898, (1981) p. 230.
- [17] T. Schreiber, Phys. Rep. 308 (1999) 1; chao-dyn/9807001.
- [18] P. Grassberger, I. Procaccia, Phys. Rev. Lett. 50 (1983) 346.
P. Grassberger, I. Procaccia, Physica D 9 (1983) 189.
- [19] J. Theiler, Phys. Rev. A 34 (1986) 2427.
- [20] M. Frank et al., Physica D 65 (1993) 359.
- [21] A. Potapov, J. Kurths, Physica D 120 (1998) 369.
- [22] F. Takens, Lecture Notes in Mathematics, Springer-Verlag, Berlin, vol. 1125, (1985) p. 99.
- [23] J. Theiler, Phys. Lett. A 135 (1988) 195.
- [24] A.R. Osborne, A. Provenzale, Physica D 35 (1989) 357.
- [25] A. Provenzale et al., Physica D 58 (1992) 31.
- [26] J. Theiler, D. Prichard, Physica D 94 (1996) 221.
- [27] J. Theiler et al., Physica D 58 (1992) 77.
- [28] T. Schreiber, A. Schmitz, Phys. Rev. Lett. 77 (1996) 635; chao-dyn/9909041.
T. Schreiber, A. Schmitz, chao-dyn/9805013.
T. Schreiber, Phys. Rev. Lett. 80 (1998) 2105; chao-dyn/9909042.
T. Schreiber, A. Schmitz, Physica D 142 (2000) 346; chao-dyn/9909037.
- [29] W. A. Brock et al., A Test for Independence Based on the Correlation Dimension (University of Wisconsin Press, Madison, 1987).

- [30] T. Schreiber, A. Schmitz, Phys. Rev. E 55 (1997) 5443; [chao-dyn/9909043](#).
- [31] T. Schreiber, Phys. Rev. E 48 (1993) R13.
- [32] A. Schmitz, T. Schreiber, Phys. Rev. E 59 (1999) 4044; [chao-dyn/9804042](#).
- [33] J.-P. Eckmann, D. Ruelle, Rev. Mod. Phys. 57 (1985) 617.
- [34] Yu.A. Fomin et al., Proc. 26th ICRC, Salt Lake City, vol. 1, (1999) p. 286.
- [35] J.W. Eaton, GNU Octave: A high-level interactive language for numerical computations (Edition 3 for version 2.0.13, 1997); <http://www.octave.org/>
- [36] J. Theiler, J. Opt. Soc. Am. A 7 (1990) 1055.
- [37] M. Ding et al., Physica D 69 (1993) 404.
- [38] J.-P. Eckmann, D. Ruelle, Physica D 56 (1992) 185.
- [39] Yu.A. Fomin et al., [astro-ph/0207190](#), v.1.
- [40] R. Hegger et al., Chaos 9 (1999) 413; [chao-dyn/9810005](#).
See also <http://www.mpipks-dresden.mpg.de/~tisean>
- [41] The BATSE Gamma Ray Burst Catalogs,
<http://www.batse.msfc.nasa.gov/batse/>
- [42] R.A. Burger, 26th ICRC, Invited, Rapporteur, and Highlight Papers, AIP Conf. Proc., vol. 516 (2000) 83.
- [43] L.F. Burlaga et al., Proc. 26th ICRC, Salt Lake City, vol. 7, (1999) p. 107.
J.S. Perko, L.F. Burlaga, J. Geophys. Research 97 (1992) 4305.
- [44] A.A. Lagutin, V.V. Uchaikin, Proc. 27th ICRC, Hamburg, vol. 2001, (5) p. 1900.
- [45] L.F. Burlaga et al., Astrophys. J. 407 (1993) 347.
L.F. Burlaga, J. Geophys. Research 97 (1992) 4283.
L.F. Burlaga, L.W. Klein, J. Geophys. Research 91 (1986) 347.
- [46] M. Chikawa et al., Proc. 24th ICRC, Rome, vol. 1, (1995) p. 277.
- [47] S. Ohara et al., Proc. 27th ICRC, Hamburg, vol. 1, (2001) p. 208.